Center-to-limb distribution of bright points and faculae: first results of an automated detection algorithm

P. Kobel, J. Hirzberger, V. Zakharov, A. Gandorfer and S. K. Solanki

Max-Planck Institute für Sonnensystemforschung, Max-Planck-Straße 2, 37191 Katlenburg-Lindau, Germany

Abstract.   Center-to-Limb variations (CLV) of photospheric Bright Points (BPs) and faculae are important to understand the fundamental relationship between these magnetic features. In this context, we present a statistical study of the center-to-limb distribution of BPs and faculae in active regions. Magnetic brightenings were detected at various disk positions by an automated segmentation algorithm based on joint G-band and continuum information. They were then classified as BPs or faculae according to a linear discriminant analysis, which allowed to determine the relative fraction of the two classes at each disk position.

1.   Introduction

It has long been known that small-scale magnetic flux concentrations (the so-called magnetic elements) appear mainly as Bright Points (BPs) near solar disk center, while faculae are their signatures near the limb. However, the fundamental relationship between these two radiative features is not yet clear: Are BPs and faculae associated with similar magnetic flux entities (size, field strength)?

Recent comprehensive 3D MHD simulations have tackled this issue, qualitatively mimicing the transition from BPs to faculae by skewing simulation boxes. However, quantitative discrepancies with observations still remain regarding the contrast values of these features, and the striations of faculae (Keller et al. (2004); Carlsson et al. (2004)).

To shed more light on the relationship between BPs and faculae, we performed a center-to-limb variation study of the relative number distribution of individual BPs and faculae, using discriminant analysis techniques on high-resolution images of active regions. Through this work, we want to provide a novel observational constraint for MHD models, as well as to give an example of application of linear discriminant analysis on solar data.

2.   Image Processing and Segmentation

Simultaneous G-band (430 ± 0.5 nm) and nearby G-continuum (436 ± 0.5 nm) images were recorded at the Swedish Solar Telescope (La Palma). They cover active regions at various disk positions in the range $< \mu > \in (0.56, 0.97)$, where $\mu \equiv \cos\theta$, θ is the heliocentric angle and $< \mu >$ is the mean value of the images. This target μ range is where the transition from BPs to faculae is believed to occur.

   Phase-diversity reconstruction allowed to achieve almost diffraction-limited images (angular resolution $\sim$ 0.1 arcsecs). Simultaneous image pairs (G-band and continuum) were first aligned using warping techniques. They were then de-rotated along the solar radial vector by comparison with MDI data, and divided by the limb darkening μ-polynomial of Neckel & Labs (1994). The resulting intensity of the image pairs was normalized by the mean intensity of a common 'quasi-quiet sun' subfield, used as reference for the definition of contrast: $C_{G,C} = (I - <I>_{QS,ref})/<I>_{QS,ref}$, where the subscript G and C stand for G-band and continuum. To remove medium and large-scale fluctuations of the intensity, we applied a high-pass spatial frequency filter with a cut-off frequency of 0.2 arcsec^{-1} (Hirzberger (2005)).

   Our photometric segmentation algorithm proceeded in two steps. First, a Multi-Level Tracking (MLT) segmentation (Bovelet & Wiehr (2003)) was applied to the G-band images, allowing to resolve BPs chains and faculae striations into individual features. Second, bright magnetic features were selected by requiring each MLT-segmented structure to contain a minimum of 5 pixels (res. limit) with values above a G-band contrast threshold and a contrast difference threshold (Berger et al. (1998)).

3.   Discriminant Analysis of Bright Points and Faculae

Prior to classify each feature as a BP or a facula, we performed a descriptive discriminant analysis to find out the combination of physical parameters that best discriminate the two classes of features. This study was performed on a *training set* consisting in 200 BPs and 200 faculae, obtained by manual selection of 40 features at five disk positions. To define discriminant parameters, we retrieved characteristic contrast profiles as follows. First, the features were oriented in a local x/y coordinate frame, such that the y-component of the G-band contrast moment of inertia is minimum. Next, averaged profiles were computed in x and y and the smoothest one was chosen, yielding *one* characteristic profile per feature (Fig 1).
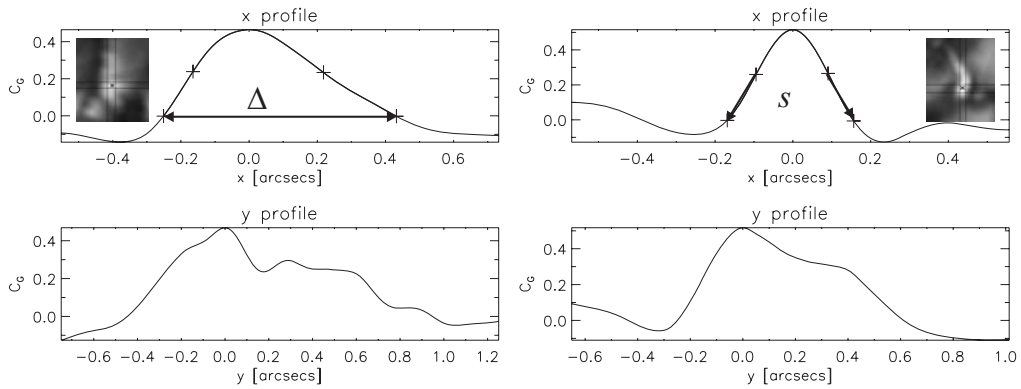

Figure 1.   (left) Average G-band contrast profiles for a typical facula. (right) Idem for a typical BP. The corner windows next to the x-profiles show the feature orientation in its local x/y coordinate frame, and the black lines delimit the pixels used for profile averaging.

Three parameters were found to be good discriminants between the BPs and faculae of the training set:

- $\Delta :=$ extent of profile at the reference level $C_G = 0$ [arcsecs]

- $s :=$ mean slope of the profile below the half-max level $C_{G,HM} = 0.5C_{G,max}$

- $A :=$ area of the feature defined by the segmentation [arcsecs^2]

We further took the logarithm of these parameters in order to reduce the skewness of their density functions. The 3 log-transformed parameters were then combined in a 3D parameter space and we applied Fischer (1936) linear discriminant analysis to find the axis of the parameter space along which the class separability is maximum. The original parameters can then be projected onto this axis by linear combination, defining a single variable F that best separates the two classes (Fig 2).
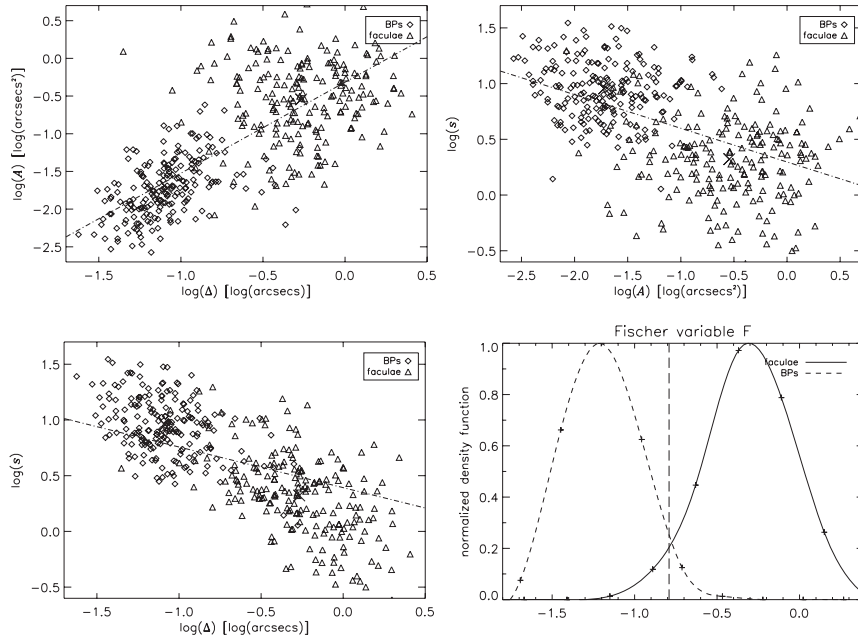

Figure 2. 2D projections of the 3D training set vectors $\{log(A), log(\Delta), log(s)\}$, together with the projected axis of maximum separability. (bottom right) Spline-interpolated density function histogram of the variable F with the BP-faculae threshold (long dashed line).

Finally, to classify BPs and faculae, we made the usual choice of a threshold value on F at equal standardized distance from the classes means. Using this threshold, all the segmented features of our dataset were classified according to their value of F. At each $< \mu >$, we calculated the fraction of BPs and faculae relative to the total number of features. The resulting fraction CLV (Fig 3) is mostly faculae-dominated with a transition from faculae to BPs at $\mu \sim 0.9$. This is consistent with 2D simulations of Steiner (2005) indicating that transcient faculae could be produced near disk center by swaying flux tubes. Conversely,

flux tubes inclined towards the line of sight may be less subject to give rise to BPs, due to the increasing foreground granular obscuration as we approach the limb. The CLV exhibits a plateau in the range $\mu \in (0.6, 0.8)$, indicating that inclined fields-induced BPs may be found in that range, but disappear further to the limb.
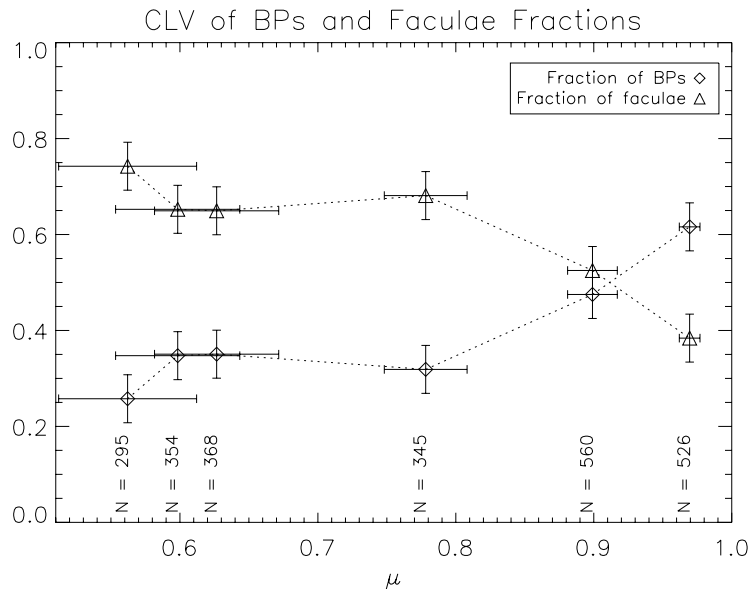

Figure 3.   Fraction of BPs and faculae relative to the total number of features N at each disk position. The horizontal error bars correspond to the μ coverage of each image.

Note that the fraction error bars are upper limit estimates of the *misclassification rates*, and do not represent statistical errors. Hence, the choice of a different dataset (e.g. in QS network) could lead to a different fraction CLV. A similar classification study could be performed on a dataset with magnetic field vector information, in order to determine the magnetic properties of BPs and faculae independently.

References

Keller, C.U., Schüssler, M., Vögler, A., & Zakharov, V. 2004, ApJ, 607, L59
Carlsson, M., Stein, R.F., Nordlund, A., & Scharmer, G. 2004, ApJ, 610, L137
Neckel, H. & Labs, D. 1994, Solar Phys., 153, 91
Hirzberger, J. & Wiehr, E. 2005, A&A, 438, 1059
Shelyag, S., Schüssler, M., Solanki, S.K., Berdyugina, S.V., & Vögler, A. 2004, A&A, 427, 335
Berger, T., Lödahl, M., Shine, R.S., & Title, A. 1998, ApJ, 495, 973
Bovelet, B. & Wiehr, E. 2003, Solar Phys., A&A, 412, 249
Fischer, R.A. 1936, Annals of Eugenics., 7, 179
Steiner, O. 2005, A&A, 430, 691